Article

Propylene Oxide Addition Effect on the Chemical Speciation of a Fuel-Rich Premixed *n*-Heptane/Toluene Flame

Artëm M. Dmitriev, Ksenia N. Osipova, Denis A. Knyazkov,* and Andrey G. Shmakov

Read Online
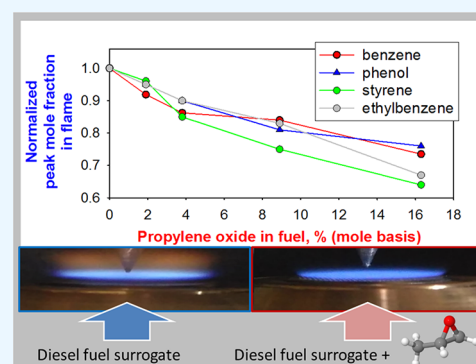
ACCESS | Metrics & More | Article Recommendations | Supporting Information

ABSTRACT: 1,2-Propylene oxide (PO, C_3H_6O) is considered as a promising agent for improving fuel. In this work, the effect of PO additives on the species pool in a premixed burner-stabilized fuel-rich (ϕ = 1.6) flame fueled by *n*-heptane/toluene mixture (7/3 by volume of liquids) at atmospheric pressure is studied by the flame-sampling molecular beam mass spectrometry and numerical modeling in order to get insight into the chemical aspects of the influence of oxygenates with an epoxy group on the formation of abundant intermediates (including PAH precursors) during combustion of fossil fuels. The flames with various loadings of PO in the fuel blend (from 0 to 16.3% in mole basis) are examined, and detailed kinetic mechanisms available in the literature are validated against the measurements of mole fraction profiles of reactants, major products, and many intermediate species. A higher reactivity of the fresh mixture and a reduction in the peak mole fractions of intermediates playing an important role in PAH formation

(benzene, styrene, ethylbenzene, phenol, acetylene, diacetylene, etc.) are observed when PO is added. This was found to be due to simultaneously two factors: the partial replacement of "sooting" fuel (toluene, which is the main precursor of these species) with oxygenated additive, and the changes in the flame radical pool caused by PO addition. Propylene oxide additive was found to change the ratio between H, OH, O, and CH_3 toward an increase in the proportion of O and CH_3. The detailed kinetic mechanisms considered in the work are found to overpredict the peak mole fraction of acetylene, a key species playing a crucial role in PAH growth. Its chemistry is revisited in order to provide a better prediction of C_2H_2 and, as a result, PAHs.

1. INTRODUCTION

Propylene oxide (PO, C_3H_6O, 1,2-propylene oxide) is an important industrial chemical that is used primarily in the synthesis of other compounds. Extensive studies are focused on the direct PO synthesis mostly from propylene.[1−4] However, the direct epoxidation of propylene appeared to be challenging due to the low selectivity of catalysts. Although considerable efforts are being made to understand the kinetics of this conversion, the detailed mechanism of the epoxidation process is still unclear.[5,6] Large-scale production of PO is often considered dangerous due to a high volatility, high flammability, and wide explosion limits of PO.[7] In this regard, it is also considered as a model and practical fuel-air explosive.[8−10] Thus, extensive experimental and numerical studies of PO/air explosion mechanisms have been carried out using simplified[11] and detailed[9] kinetic schemes.

Particular attention was paid to PO thermal decomposition, oxidation, and combustion kinetics, because propylene oxide is an important intermediate formed during the oxidation of other hydrocarbons.[12,13] Lifshitz and Tamburu[14] studied PO decomposition and ring opening by measuring the products formed behind the reflected shock waves in the PO/Ar mixture in a single-pulse shock tube. They proposed a reaction scheme for PO isomerization and thermal decomposition. Later Burluka et al.[15] measured the laminar burning velocities of

C_3H_6O isomers (PO, propanal, and acetone) in air at atmospheric pressure. Propylene oxide was found to burn faster than its isomers. A new kinetic scheme was proposed to simulate the data obtained, but quantitative agreement between measurements and predictions of PO/air flame speed was not reached.

The experimental and numerical characterization of the chemical structure of one-dimensional premixed burner-stabilized laminar PO/O₂/Ar flames was reported by Knyazkov et al.[16] The authors have measured spatial distributions of mole fractions of reactants, major products, and various intermediates in the flames with different equivalence ratios using flame sampling molecular beam mass spectrometry (MBMS). Three kinetic models with different detail levels were validated against the measurement data. It was shown that the branching ratio between the isomerization pathways of PO should be revisited.

Table 1. Molar Composition of the Reactant Mixtures

flame	n-heptane/toluene/PO ratio (by vol. of liquids)	PO content in fuel blend, % (mole basis)	mole fraction, %				
			n-heptane	toluene	PO	O_2	Ar
A (base flame)	7:3:0	0	2.12	1.26	0	21.63	75
B	7:3:0.1	1.9	2.10	1.25	0.07	21.59	75
C	7:3:0.2	3.8	2.08	1.24	0.13	21.56	75
D	7:3:0.5	8.9	2.02	1.20	0.32	21.46	75
E	7:3:1	16.3	1.94	1.15	0.60	21.31	75

Ramalingam et al.[17] have investigated PO reactivity at low and intermediate temperatures in a series of shock tube and rapid compression machine experiments. Ignition delay times were measured at different stoichiometries and pressures. Kinetic analysis revealed vital sections for the improvement of the model like the ketene subchemistry and pathways leading to the formation of benzene.

Since PO is produced in large industrial scales and could be easily transported, it was proposed as an oxygenated additive to transportation fuels[18,19] to reduce soot content in the exhaust of diesel engines. Recent study has shown that there is no evidence that typical environmental or occupational exposures to PO constitute a health risk for humans.[20] Therefore, the use of PO as a fuel-improving agent may be promising.

It is well-known that PAHs and soot are formed in flames of oxygen-containing fuels in smaller amounts than in flames of hydrocarbons of comparable molecular weight.[21,22] This suggests using oxygenates as PAH and soot-reducing additives to traditional fuels. It was shown that the ability of oxygenates to influence the pathways of PAHs and soot formation depends not only on the number of oxygen atoms in a molecule but also on the chemical structure of the molecule itself.[23−26] In this regard, many studies have been devoted to the search and testing of oxygenated additives among alcohols, ethers, esters, and ketones.[27] Various representatives of these classes have been studied, either as individual fuels or as additives to the conventional hydrocarbon fuels. Thus, the search for an optimal oxygen-containing fuel/additive has become a current research hotspot. At present, it is mainly based on an understanding of the combustion chemistry of these compounds. From this point of view PO looks attractive since in flames it mostly isomerizes to acetone and propionaldehyde and therefore can act as a blend of two classes of oxygenates: ketone and aldehyde. However, to our knowledge, there are no studies of the effect of PO additives on soot and PAH formation during combustion of hydrocarbon fuels.

Therefore, this work is focused on experimental and numerical investigation of the effect of PO addition on the species pool in a premixed burner-stabilized fuel-rich flame fueled by n-heptane/toluene mixture. Examining this model system in laboratory conditions, we aim to get insight into the chemical aspects of influence of oxygenates with an epoxy group on formation of abundant intermediates (including PAH precursors) during combustion of fossil fuels. Similar to the previous works,[28−31] a mixture of n-heptane and toluene with fixed ratio of these constituents (7/3 by volume of liquids) is considered here as a surrogate of diesel fuel. Spatial distributions of various species in the flames fuelled by the n-heptane/toluene mixture with addition of different amounts of PO are measured using the flame-sampling molecular beam mass spectrometry and simulated with the detailed chemical kinetic mechanisms available in the literature. Since the

uncertainty in MBMS measurements of the absolute mole fractions of many intermediates in flames is quite high (up to ∼ ± 50%), the ratio of the peak mole fraction of a certain intermediate in the flame with and without PO addition (which is determined with decreased uncertainty) is used in this work as a target for validation of the kinetic models. Performances and deficiencies of the kinetic models in prediction of the observed tendencies are discussed. Kinetic analysis is also conducted in order to elucidate if the effect of PO on PAH precursors is due to partial replacement of "sooting" fuel with oxygenated additive or due to chemical interactions between the primary oxidation products of different fuels.

2. EXPERIMENTAL DETAILS

The flames of n-heptane/toluene/O_2/Ar mixtures with and without propylene oxide addition stabilized on a Botha−Spalding type burner[32] at atmospheric pressure have been investigated in this work. The burner and the mixture preparation system have been thoroughly described earlier;[33] thus, only essential details are given below.

The matrix of the burner represented a perforated disc (0.5 mm orifices with 0.7 mm center-to-center spacing) 16 mm in diameter and 3 mm thick, which was screwed into the brass body of the burner. The burner temperature was kept at 95 °C by thermostated water circulating through the water jacket in the burner body. A fresh gaseous mixture consisting of gaseous oxygen, argon, and vapors of n-heptane and toluene was supplied into the burner from the electrically heated vaporizer via a heated line. n-Heptane and toluene were blended in a ratio of 7:3 (by volume of liquids) and supplied into the vaporizer through a steel capillary using a syringe pump driven by a stepper motor. The temperature of the vaporizer was kept at 90 °C. The flow rates of gaseous oxygen and argon were regulated by calibrated mass-flow controllers (Bronkhorst). Propylene oxide has a significantly lower boiling temperature (34 °C at 1 bar) as compared to that of toluene and n-heptane; thus, it was supplied from a separate syringe pump via a hypodermic needle directly into the heated line connecting the vaporizer and the burner. This made it possible to ensure a stable supply of highly volatile propylene oxide to the unburnt mixture.

Fuel-rich, but nonsooting, laminar premixed flames with the following parameters kept unchanged have been investigated in this work:

- n-heptane/toluene ratio: 7:3 by volume of liquids, which is equivalent to their ratio of 1.68 in mole basis;
- equivalence ratio: $\phi = 1.6$;
- argon content in the mixture: 0.75 in mole basis;
- total mass flow rate of unburnt mixture: 0.0133 g/cm^{3}s.

The flame conditions differed in the content of propylene oxide in the fuel mixture. The ratio of liquid volumes of n-

heptane/toluene/PO was varied from 7:3:0 to 7:3:1. Oxygen content was also adjusted correspondingly to maintain the same equivalence ratio $\phi = 1.6 \pm 0.02$. The procedure on how the uncertainty in the equivalence ratio determination was estimated is given in the Supporting Information. In total, 5 flames have been examined with PO variation from 0% to 16.3% in mole basis in fuel mixture; their molar composition is given in Table 1.

Mole fractions of various species in the flames were measured as a function of the height above the burner (HAB) using flame-sampling molecular beam mass spectrometry (MBMS) with soft ionization by electron impact. The experimental apparatus was thoroughly described earlier and used in studies of chemical speciation of flames of liquid fuels.[33−36] Therefore, only essential details are provided in the following.

Gas sampling was performed using a quartz conical probe with an inner opening angle 40° and an orifice diameter of 0.08 mm. The wall at the nozzle tip had a thickness of 0.08 mm. Behind the sampling probe, sampled gases formed a molecular beam, which passed through a skimmer and a collimator and entered the area of soft ionization by electrons emitted from a tungsten filament. Compensation of voltage drop on the filament allowed the spread in the electron energies to be defined only by thermal distribution (fwhm ≈ 0.5 eV). The energy of ionizing electrons (which could be varied in the range of 8−20 eV) was selected individually for each species so that, on the one hand, it was higher than the ionization energy and provided a reasonable signal-to-noise ratio, and, on the other hand, not high enough to cause the contribution of fragmented ions from other species. The ions formed were analyzed by a quadrupole mass spectrometer MS 7302. The burner was mounted on a translation mechanism to manually vary its vertical position (with the accuracy of $\sim\pm10~\mu m$) and to scan over the distance between the burner surface and the sampling probe tip. This allowed sampling the flames and recording the signal intensities of the mass peaks of interest at different heights above the burner (HAB).

The species detected in the flames are listed in Table S1, which shows also the electron energies used, the calibration method applied in this work, and the uncertainty in determination the mole fractions for each species. The calibration factors used to convert measured mass peak intensities to the species mole fractions have been determined according to the procedures thoroughly described in our earlier works.[34,36,37] Briefly, the following two calibration methods were used: direct calibration method (using gas mixtures of known composition) and relative ionization cross-section (RICS) method proposed by Cool et al.[38] (for radicals and species for which gas mixtures were not feasible).

To eliminate the uncertainties induced by instrumental inconstancies,[39] the measurements in all flames have been carried out in the same experimental run. The following three main sources of uncertainties in the mole fraction evaluation can be distinguished: (1) the statistical error of the measurement of the mass peak signals in the flame, (2) the error in the determination of calibration coefficients, which depends on the calibration method used, and (3) the degree of reliability in the separation of the contributions from parent or fragmentary ions of other species. Typical measurement error (relative standard deviation) of signal intensities of most mass peaks relevant to this work was as a rule below 10%. Therefore,

a relative comparison of mole fraction of each species from different flames offers a precision within $\sim$10%.

Flame disturbances are inevitable when using conical nozzles for gas sampling. However, extensive studies carried out earlier[40−45] have shown that hydrodynamic perturbations caused by the probe mainly due to gas suction may be corrected by shifting the measured species mole fraction profiles upstream to the burner. Similarly to as was done in previous works focused on flame structure measurements,[16,30,33,46] in this study all experimental mole fraction profiles in each flame were shifted toward the burner by the same distance (0.2 mm) to superpose the peak values of the water mole fraction and temperature profiles.

The "disturbed" flame temperature profiles were measured by an S-type thermocouple made of wires 0.03 mm in diameter and coated with SiO_2. During the measurements, the thermocouple junction was located 0.2 mm upstream of the probe tip. Corrections for radiation heat losses by the thermocouple were made according to the procedure described earlier.[47,48] The maximum uncertainty in the temperature measurements did not exceed ± 60 K. All experimental data (temperature and species mole fraction profiles) reported in this work are tabulated in the Supporting Information.

3. MODELING

Chemical structures of the laminar one-dimensional premixed flames studied experimentally in this work were simulated using the PREMIX code from the CHEMKIN II package. The calculations were carried out using the "burner-stabilized flame" option in the PREMIX code simulations. The temperature profiles measured in a manner described above were used as input to account for the flame cooling effects by the sampling probe.

Propylene oxide is usually ignored in detailed chemical kinetic models for surrogate fuels, since it is a much less abundant C_3H_6O intermediate in contrast with its isomers, acetone and propanal. There are only few detailed chemical kinetic mechanisms available in the literature, which involve simultaneously all reactants presented in the fuel blend studied in this work (n-heptane, toluene, propylene oxide). To the best of our knowledge, they are (1) the kinetic mechanism provided by CRECK Modeling at Politecnico di Milano[49] and (2) C3MechV3.3 (3761 species and 16 522 reactions), a detailed kinetic model for surrogate fuels developed by the Computational Chemistry Consortium research team.[50] Both mechanisms are hierarchically organized and self-consistent. They contain detailed chemistry for small species (including many oxygenates, and PO is among them) and important surrogate fuel components for jet fuel, diesel, gasoline, including PAHs. These mechanisms were used for kinetic modeling of the flames in this work.

Recently, three different mechanisms for PO combustion kinetics[51−53] with different level of detail were validated against the MBMS data for the chemical structure of premixed burner-stabilized $PO/O_2/Ar$ flames.[16] Among all the mechanisms, the kinetic mechanism of Capriolo et al.,[51] incorporating the most of PO decomposition pathways including isomerization to propanal and acetone, demonstrated a generally good predictive capability.

This motivated us to also use it in the current work for further validation against the new experimental data. The mechanism of Dirrenberger et al.[29] was chosen as a base

kinetic mechanism describing combustion kinetics of the *n*-heptane/toluene mixture, similarly as was done previously.[30,31,36] Therefore, the specific intermediates and reactions from the mechanism of Capriolo et al.[51] were incorporated to the mechanism of Dirrenberger et al.[29] to model the flames with propylene oxide additive. The resultant mechanism (hereinafter denoted as D+K) involves 313 species and 2258 reactions.

4. RESULTS AND DISCUSSION

This Section is organized as follows. First, the effect of PO additive on temperature and mole fraction profiles of major flame species (reactants and final products) is discussed. Then, the influence of partial replacement of fuel with PO on the mole fraction profiles of primary aromatic intermediates, major flame radicals, and small hydrocarbon intermediates is considered, and performances and deficiencies of the kinetic mechanisms in predicting the observed tendencies are discussed. Finally, some improvements to the chemistry of acetylene, the major intermediate playing a crucial role in PAH growth, are suggested, and a modified kinetic mechanism is validated against the experimental data.

4.1. Temperature and Major Flame Species. Figure 1 shows the temperature profiles measured in the base flame
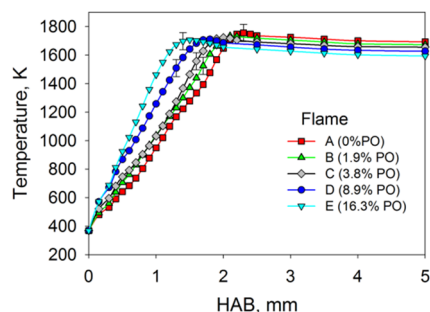
Figure 1. Temperature profiles measured in the flames with different loading of PO in the fuel blend.

(Flame A) and the flames with different amount of PO in fuel mixture (Flames B−E). As is seen, the width of the flame zone determined as the HAB where maximum temperature is attained becomes narrower with the PO loading in the fuel

mixture; i.e., the flame with higher PO content in the mixture tends to stabilize closer to the burner. This indicates the fact that the flame speed rises as the PO content in the unburnt mixture increases, which is quite expected because of higher laminar burning velocity of PO[15] as compared to those of *n*-heptane and toluene.[29] Thus, the addition of PO enhances combustion of the base fuel. Nevertheless, as seen from Figure 1a, the postflame temperature gradually decreases with the rise of PO loading (up to ∼110 K when 16.3% of the base fuel is replaced with PO), because as the flame gets closer to the burner, heat losses to the burner increase.

In Figure 2, mole fraction profiles of the major species (*n*-heptane, toluene, PO, oxygen, water, CO, CO_2, and H_2) measured in the base flame (Flame A) and the flame with addition of 8.9% of PO in the fuel blend (Flame D) are compared with the predictions by different detailed kinetic mechanisms. As seen, all three mechanisms adequately reproduce the experimental data and provide very similar predictions of the profiles. Both experiment and modeling show that addition of PO does not result in any notable change in the postflame mole fractions of CO, CO_2, H_2O, H_2. It can also be seen from Figure 2 (as well as from Figure1) that the flame zone becomes narrower with addition of PO in fuel.

4.2. Primary Aromatic Intermediates. Mole faction profiles of some aromatic intermediates (benzene, phenol, styrene, and ethylbenzene) measured in the flames with and without PO addition are compared in Figure 3 with those simulated using different detailed chemical kinetic mechanisms. As seen, in general, all three mechanisms give reasonable description of these experimental profiles in all flames: the HAB where the peak mole fractions are attained and also the shape of the profiles are predicted fairly well. There are, however, some insignificant discrepancies between the predictions and measurements of the peak mole fractions of these species. Particularly, benzene peak mole fraction is only slightly overpredicted by all mechanisms, phenol peak mole fraction is overestimated by the D+K mechanism, whereas styrene peak mole fraction is predicted precisely only by D+K and CRECK mechanisms. As seen from the experimental data presented in Figure 3, addition of up to 16.3% of PO to the fuel blend results in some changes in the peak mole fractions of these aromatic intermediates, which are however within the uncertainty in the determination of the
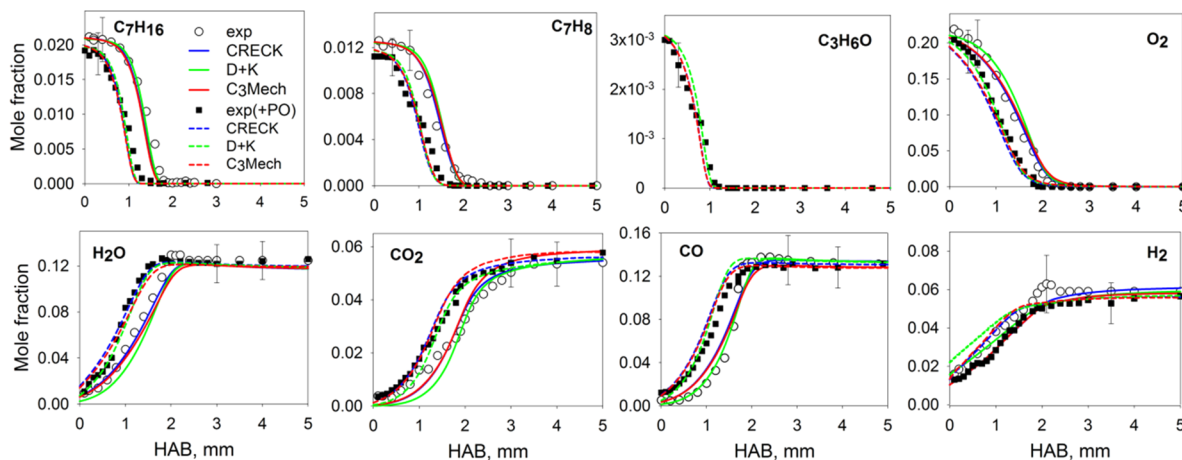
Figure 2. Measured (symbols) and simulated (lines) mole fraction profiles of the reactants and major products in the flames. Base flame (Flame A): open symbols and solid lines. Flame with addition of 8.9% PO in fuel (Flame D): filled symbols and dashed lines.
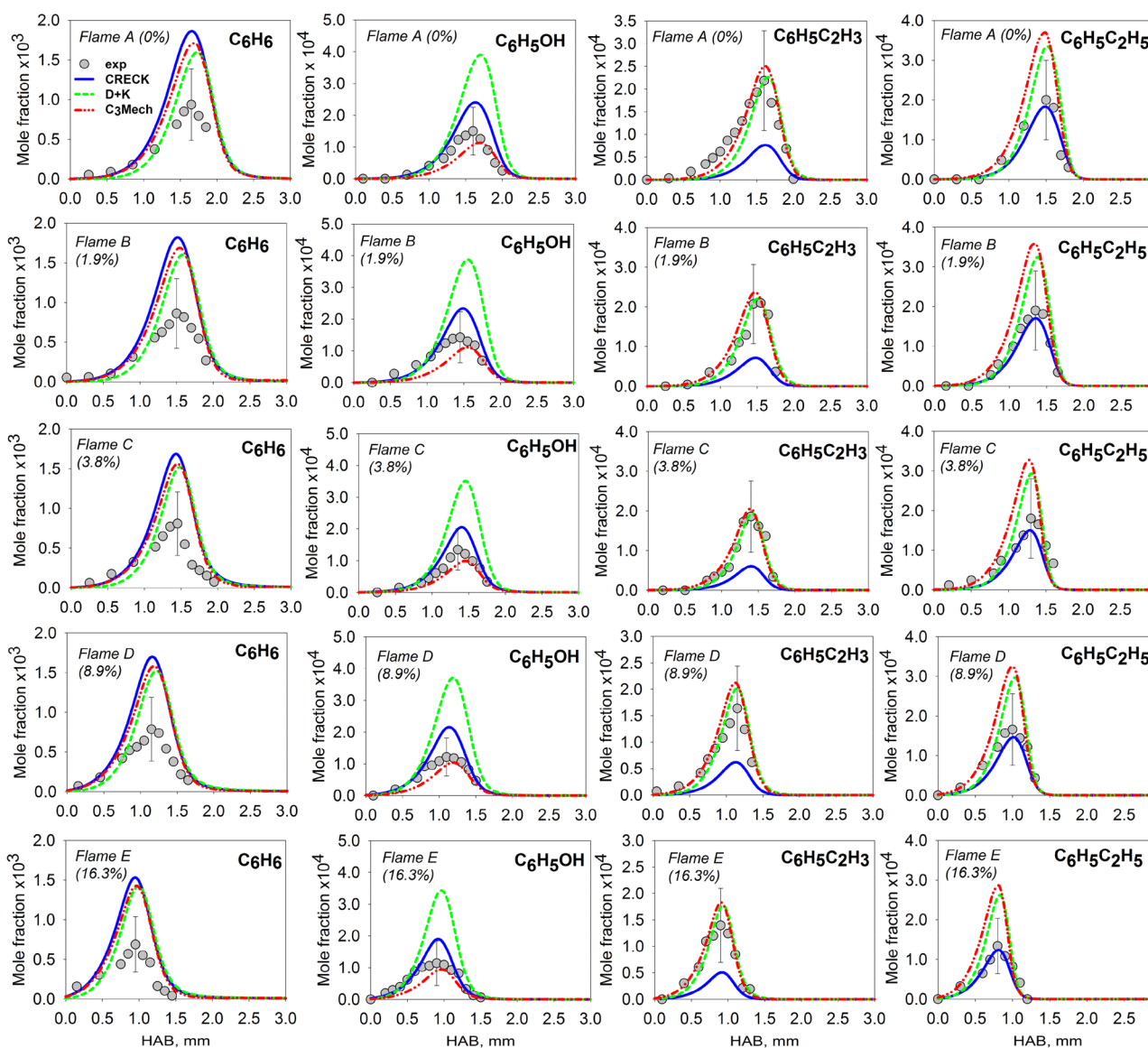
Figure 3. Measured (symbols) and simulated (lines) mole fraction profiles of some aromatic intermediates (benzene, phenol, styrene, ethylbenzene) in the base flame (Flame A) and in the flames with different loading of PO (1.9%, 3.8%, 8.9%, 16.3% in fuel: Flames B−E, respectively).

absolute mole fractions. Nevertheless, these experimental data can be used to assess the effect of PO addition on the relative change in the species maximum mole fractions, which was measured with higher precision (see Experimental Details section).

Both experiment and modeling showed that the higher content of PO in the fuel blend, the lower is the peak mole fractions of these intermediates in the flame. To clearly demonstrate this fact, in Figure 4, we plotted normalized peak mole fractions of these four species (calculated as a ratio of the peak mole fraction of a particular intermediate in the flame with PO to that in the base flame) versus the percentage of PO in the fuel blend. As seen from this figure, all three mechanisms provide quite reasonable reproduction of the effect of PO additive in terms of relative reduction of the maximum mole fractions of the aromatic intermediates in the flame of *n*-heptane/toluene mixture. Nevertheless, CRECK mechanism and C3Mech provide a better agreement with the experimental data.

Both experiment and simulations show that the effect of PO additive on these species is linear with PO loading, at least up to ~16% of PO in fuel. If this effect was due exclusively to the partial replacement of "sooting" fuel (toluene) with oxygenated additive, then (all other conditions being equal) one would expect that the PO influence to the peak mole fractions of all the considered aromatic intermediates would be the same. However, according to measurements, benzene and phenol peak mole fractions are reduced by ~25 ± 3%, whereas styrene and ethylbenzene are reduced by 36 ± 4% and 33 ± 4%, respectively, when 16.3% PO is added in fuel. As seen from Figure 4, all mechanisms also predict the same tendency. In order to reveal the reasons for such behavior and, therefore, to understand the influence of PO on the kinetics of formation of these species, we analyzed (1) the temperature at which the peak mole fractions of these species in the flames are reached (T_{peak}), and (2) the reaction pathways of formation of these species in the flame with and without PO additive.
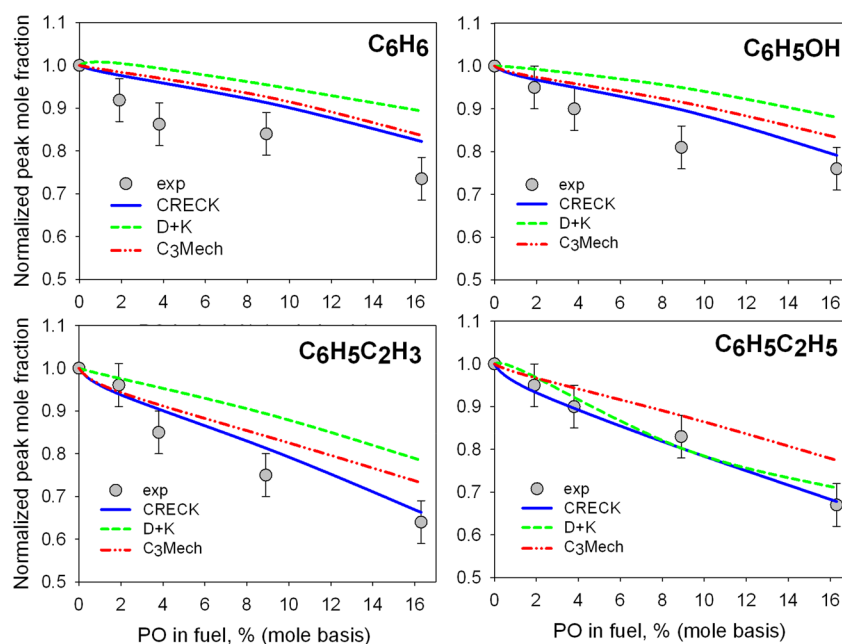
Figure 4. Normalized peak mole fraction of benzene (C_6H_6), phenol (C_6H_5OH), styrene ($C_6H_5C_2H_3$), and ethylbenzene ($C_6H_5C_2H_5$) vs the content of PO in the fuel blend.

Figure 5 shows the T_{peak} plotted versus the PO content in the fuel mixture (exemplarily, according to CRECK mecha-
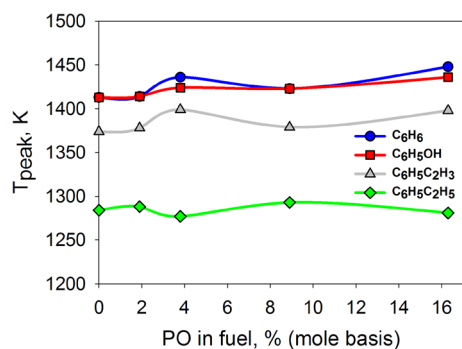

Figure 5. Temperature, at which the maximum peak mole fractions of some aromatic intermediates (see the legend) is reached in the flames, plotted vs PO content in the fuel mixture (according to CRECK mechanism).

nism). As seen, in all flames this temperature is nearly the same for a particular species, and it varies only within ±15 K. The dependencies shown in Figure 5 clearly demonstrate the order (from the burner) in which these aromatic intermediates form in the flames without and with PO: ethylbenzene → styrene→ phenol and benzene. The fact that the amount of PO loading does not influence this order may indicate that PO and its primary decomposition products have no effect on the chemistry of primary pathways of toluene oxidation, since all these intermediates are expected to be mainly the products of toluene decomposition.

Figure 6 schematically summarizes the major reaction pathways of formation of these intermediates from toluene, as derived from the rate-of-production analysis in the flame without PO additive according to C3Mech at the temperatures corresponding to particular T_{peak} values shown in Figure 5 (e.g., 1420 K for benzene). This schematic does not indicate the percentage contribution of each pathway to the total rate of

production of corresponding intermediate, because it slightly varies when switching between flames with different amount of PO additive. Analysis of other kinetic mechanisms considered in this work provides very similar structure of reaction pathways.

As seen from Figure 5, among all these intermediates, ethylbenzene peak mole fraction is reached at the lowest temperature in the flames (~1285 K), and it is obvious, because, according to all chemical kinetic mechanisms considered in this work, this intermediate is generally formed virtually directly from toluene via the formation of benzyl radical (C_7H_7):

$$C_7H_8 + H \leftrightarrow C_7H_7 + H_2 \qquad (1)$$

$$C_7H_7 + CH_3 \leftrightarrow C_6H_5C_2H_5 \qquad (2)$$
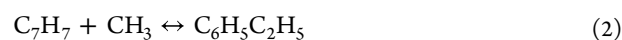
Styrene mole fraction peaks at a higher temperature (~1385 K), because its main precursor is 1-phenylethyl radical ($C_6H_5C_2H_4$), which is formed during H-abstraction from ethylbenzene:

$$C_6H_5C_2H_5 + H \leftrightarrow C_6H_5C_2H_4 + H_2 \qquad (3)$$

$$C_6H_5C_2H_4 \leftrightarrow C_6H_5C_2H_3 + H \qquad (4)$$
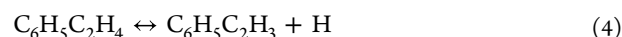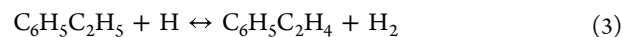
Noteworthy that benzene and phenol peak mole fractions are attained at even higher temperature (~1420 K) although it would seem that there are all the prerequisites for their formation practically directly from toluene, particularly for benzene, via the reaction of CH_3 abstraction:

$$C_7H_8 + H \leftrightarrow C_6H_6 + CH_3 \qquad (5)$$
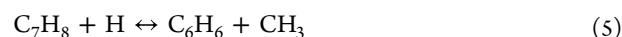
Nevertheless, according to all three models, a decomposition of 2-methyl-phenoxy radical contributes to a greatest extent to benzene formation:

$$OC_6H_4CH_3 \leftrightarrow C_6H_6 + H + CO \qquad (6)$$
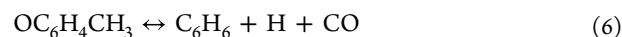
This radical in all the mechanisms is formed via the following chain of transformations:

Figure 6. Major reaction pathways of formation of ethylbenzene, styrene, phenol, benzene in the flames (according to C3Mech).

Figure 7. Measured (symbols) and simulated (lines) mole fraction profiles of the major flame radicals. Base flame (Flame A): open symbols and solid lines. Flame with addition of 8.9% PO in fuel (Flame D): filled symbols and dashed lines.

$$\text{toluene} \xleftrightarrow{+H,OH/-H_2,-H_2O} C_6H_4CH_3 \xleftrightarrow{+O_2,-O} OC_6H_4CH_3 \tag{7}$$

where $C_6H_4CH_3$ is 2-methylphenyl radical.

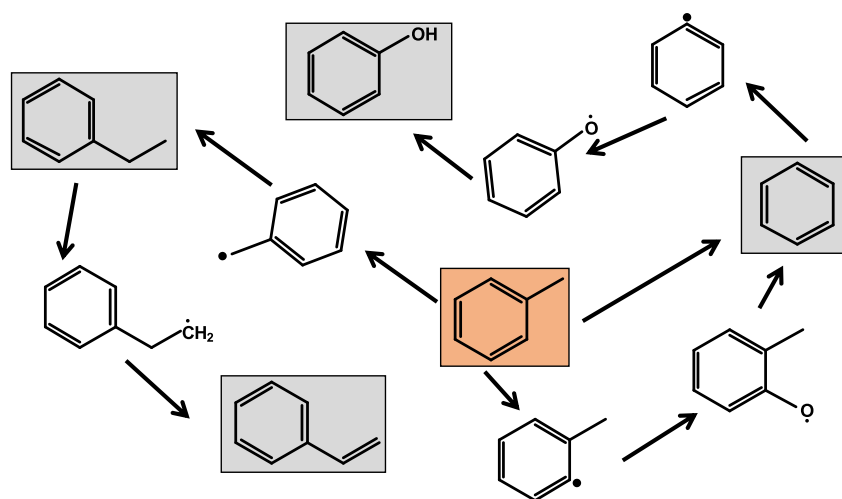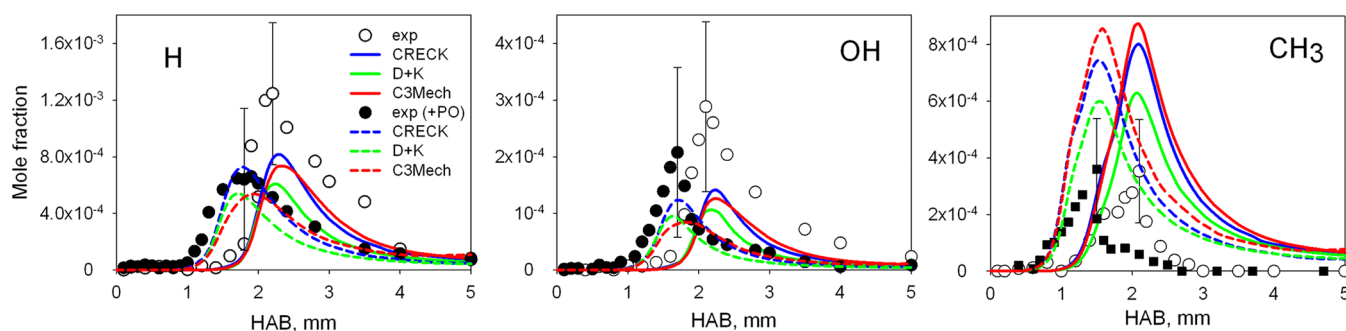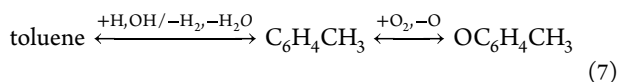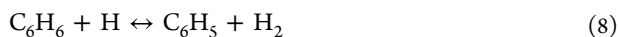Phenoxy radical (C_6H_5O) is the main precursor of phenol due to the reaction of H addition: $C_6H_5O+H\leftrightarrow C_6H_5OH$, while C_6H_5O radical is formed mainly via the following chain of reactions:

$$C_6H_6 + H \leftrightarrow C_6H_5 + H_2 \tag{8}$$

$$C_6H_5 + O_2 \leftrightarrow C_6H_5O + O \tag{9}$$

Therefore, the fact that the predictions of the effect of PO addition on the peak mole fraction of such intermediates like ethylbenzene, styrene, phenol, and benzene are in good agreement with our measurements (Figure 5) indicates the validity of the reaction pathways mentioned above in the flames of n-heptane/toluene mixture with and without the addition of PO.

4.3. Major Flame Radicals. The "chemical" effect of PO additive may be due to its influence on the pool of major flame radicals (H, O, OH, CH₃), playing a crucial role in fuel conversion in flame conditions (as also seen from the above analysis). Since addition of PO to the fuel blend enhances combustion of the mixture, this may have a notable effect on the ratio of the abundances of these radicals, because their concentrations are determined by the balance in the reactions of chain branching (e.g., $H+O_2 \leftrightarrow OH+O$), chain propagation, chain termination, and heat release ($CO+OH \leftrightarrow CO_2+H$). In

order to validate the kinetic mechanisms in their ability to predict the effect of partial replacement of parent fuel with PO on the major flame radicals, we compared the predictions with the measurements of H, OH, and CH₃ mole fraction profiles (Figure 7). As seen, all three models adequately capture the shape of the profiles, and taking into account the difficulties and high uncertainties in measurements of the radicals, one can observe a fairly good agreement between predictions and observations of the peak mole fractions of H, OH, and CH₃ in the flame without PO. All mechanisms predict a reduction in H and OH peak mole fractions, whereas CH₃ maximum abundance remains practically unchanged when PO is added. As seen, the experimental observations demonstrate the similar tendency. Although PO addition enhances the combustion of the fuel studied, the H and OH abundances decrease due to increased heat losses into the burner.

Unfortunately, we could not measure O mole fraction profiles in the flames, since this is a challenging task due to the difficulties in separating O from methane (a major intermediate), having the similar m/z ratio and close ionization energies (13.6 and 14.25 eV, respectively). Thus, in Figure 8 we present the calculated O mole fraction profiles only. As is seen, all three mechanisms predict quite low ($\sim 2.5-2.7 \times 10^{-5}$) and virtually unchanged peak mole fraction of this radical when switching from the base flame to the flame with 8.9% PO. Therefore, summarizing the obtained results on the effect of PO on the flames radicals, one can conclude that propylene oxide additive changes the ratio between H, OH, O, and CH₃
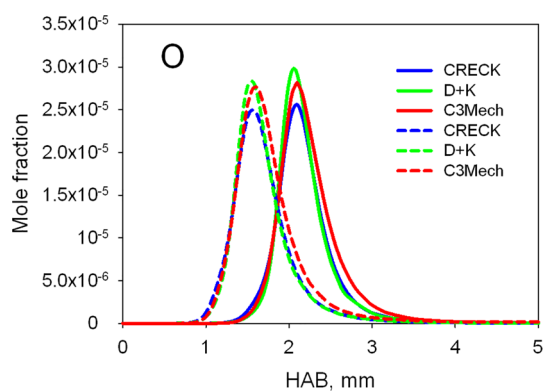
Figure 8. Simulated mole fraction profiles of O radical in Flame A (solid lines) and Flame D (dashed lines).

toward an increase in the proportion of O and CH_3. This in turn cannot but affect the concentrations of other compounds.

4.4. Small Hydrocarbon Intermediates. Addition of PO may result in significant changes in the mole fractions of small hydrocarbons, which are believed to be important species involved in the reactions of formation of PAH (see recent reviews, e.g.,[54]). We analyzed the main reaction pathways responsible for formation of cyclopenta[c,d]pyrene radical ($C_{18}H_9$), one of the heaviest PAH included in the detailed kinetic mechanism C3MechV3.3 (the schematic of these reaction pathways is shown in Figure S1). Figure S1 clearly shows that the species with one aromatic ring serve as precursors for formation of intermediates with 2, 3, and more aromatic rings. Small hydrocarbons involved in the corresponding reactions of PAH growth, like acetylene, propargyl radical, allene, propyne, cyclopenadienyl (C_5H_5), are also indicated in the diagram in Figure S1. Adequate prediction of mole fractions of these hydrocarbons in the flames with PO

addition is of particular importance to reliably describe the chemistry of PAH formation during combustion of fuel blends with addition of propylene oxide.

This motivated us to validate the chemical kinetic mechanisms against our experimental data for C1−C4 intermediate hydrocarbons detected in the flames with and without PO addition. A comparison of predicted and measured mole fraction profiles of these intermediates in the base flame and, exemplarily, in the flame with 8.9% PO in fuel blend (Flame D) is shown in Figure 9. The species corresponding to mass peaks 40 (allene+propyne) and 42 (ketene+propene), 56 (1-butene+2-butene+acrolein) were not separated due to very low difference between the ionization energies of corresponding components (see Table S1), so their summarized mole fraction profiles are represented in Figure 9.

In general, all three mechanisms give reasonable prediction of these experimental profiles in the base flame: the HAB where the peak mole fractions are attained and also the shape of the profiles are predicted fairly well for most species. However, a qualitative discrepancy between the predictions and measurements can be seen for methane (CH_4) and acetylene (C_2H_2) mole fraction profiles: all three models predict a nonzero concentration of these intermediates in the postflame zone, while their complete consumption is observed in the experiment. This disagreement for methane and acetylene in the postflame zone in fuel-rich atmospheric-pressure premixed flames is a well-known difficulty encountered earlier,[30,31,34,50,55−57] indicating that methane and acetylene chemistry in fuel-rich flames still needs to be further improved. Particular attention should be paid to acetylene chemistry, since, as clearly seen from Figure 8, it pays a crucial role in PAH growth reactions (basically according to the H-abstraction-carbon (acetylene) addition (HACA) mechanism[54,58,59])
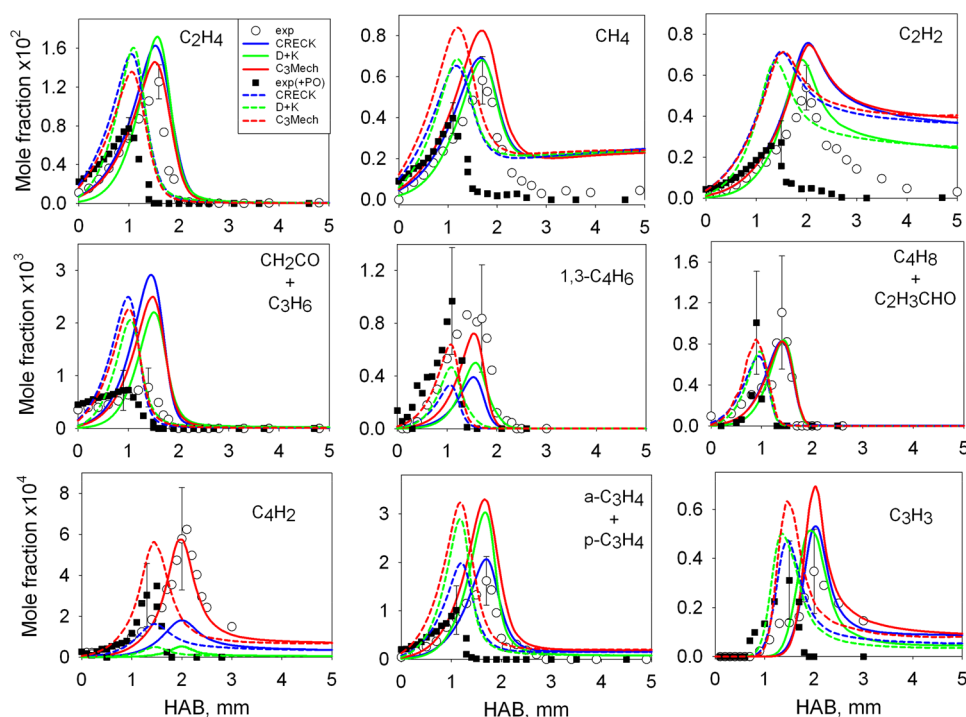

Figure 9. Measured (symbols) and simulated (lines) mole fraction profiles of C_1−C_4 intermediate products in the flames. Base flame (Flame A): open symbols and solid lines. Flame with addition of 8.9% PO in fuel (Flame D): filled symbols and dashed lines.

As seen from Figure 9, the addition of 8.9% PO to the fuel mixture does not result in any notable change in the peak mole fractions of such intermediates, like propargyl, ketene +propene, 1-butene+2-butene+acrolein. In this regard, the predictions by all three models and the experimental observations are in good agreement with each other. Noteworthy that all the mechanisms also predict the peak mole fractions of other intermediates (methane, acetylene, ethylene, allene+propyne and diacetylene) to be practically unchanged when 8.9% PO is added to the fuel mixture, as compared to the base flame. However, the measured peak mole fractions of methane, acetylene, ethylene, allene+propyne and diacetylene significantly decrease (by nearly 2 times) with the replacement of 8.9% of fuel with PO. Noteworthy that in the fuel-rich burner-stabilized flames fuelled by pure PO,[16] the kinetic mechanisms available in the literature for propylene oxide[51−53] also overpredicted methane, ethylene, and acetylene peak mole fractions. Thus, we can conclude that the discrepancies for small hydrocarbons observed in this and earlier[16] works can be explained by (1) the deficiencies of propylene oxide primary decomposition submechanisms used in the kinetic models, and (2) the deficiencies of the core hydrocarbon submechanisms used in the models.

4.5. Refinement of Acetylene Chemistry. Understanding the chemistry of formation and consumption of acetylene is of particular importance to correctly predict the formation of PAH in the flames. In this relation, here we focused on revealing the reaction pathways that should be revised to improve predictive ability of the kinetic models. For this purpose, first of all, we carried the sensitivity analysis to elucidate the reactions to the rate constants of which the acetylene mole fraction is sensitive in the flames with PO but not sensitive in the base flame.

Figure 10 shows the C_2H_2 sensitivity coefficients calculated for the height above burner of 2 and 1.5 mm corresponding to
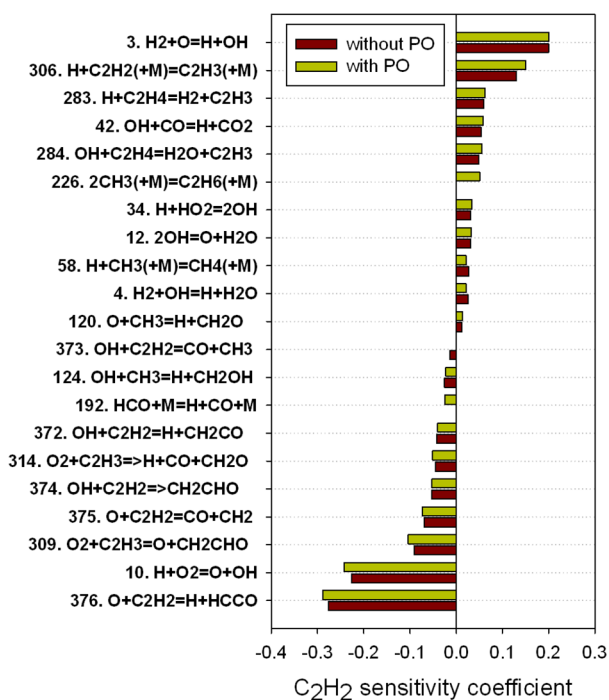
peak mole fraction of acetylene in the flames without and with 8.9% PO in fuel (Flame A and Flame D, respectively). As seen, the peak mole fraction of C_2H_2 has a significant sensitivity to the reactions involving oxygen atom: $H_2+O\leftrightarrow H+OH$, $H+O_2\leftrightarrow O+OH$, and $O+C_2H_2\leftrightarrow H+HCCO$, since the reactions of acetylene with O atoms play a key role in C_2H_2 consumption (in particular, the latter one) in the flames. The C_2H_2 peak mole fraction is also very sensitive to the reaction $H+C_2H_2(+M)\leftrightarrow C_2H_3(+M)$, which plays an important role in acetylene formation. It is particularly remarkable that in the flame with PO addition almost all reactions shown in Figure 10 have higher sensitivity coefficients than in the flame without PO, which is most likely related to the changes in the ratio between the flame radicals noted in Section 4.3. Besides, C_2H_2 peak mole fraction is much more sensitive to the reactions $HCO+M = H+CO+M$ (with a negative sensitivity coefficient) and $2CH_3(+M)\rightleftharpoons C_2H_6(+M)$ (with a positive sensitivity coefficient) in the flame with PO than in the base flame, in which their sensitivity coefficients are negligible. This can also be associated with the increased relative fraction of methyl radicals in the flame with PO, which also was discussed in Section 4.3. Therefore, an improvement of chemistry of formation of methyl, formyl and ethane in the PO submechanism may probably help to provide more accurate prediction of acetylene in the flames fueled by the blends with PO.

To check this idea, we carried out an analysis of the key reaction pathways of PO transformation to these small hydrocarbons in the flame of triple n-heptane/toluene/PO fuel blend. For the sake of brevity, the primary PO decomposition pathways constructed basing on the rate of production (ROP) analysis in the flame with addition of 8.9% PO in fuel (Flame D) are given and discussed in the Supporting Information. Summarizing the results of this analysis, we come to a conclusion that PO presence in the flames favors to rapid formation of CH_3, C_2H_5, and HCO radicals. Since PO is dominantly consumed in the flame via the isomerization to propanal and acetone, propanal largely serves as a precursor of HCO and C_2H_5 radicals, whereas acetone mainly decomposes to form CH_3 radicals. This explains the positive sensitivity coefficient of C_2H_2 to $2CH_3(+M)\leftrightarrow C_2H_6(+M)$ reaction and the negative one to the reaction involving HCO: $HCO+M\leftrightarrow H+CO+M$ (Figure 10). Thus, a more accurate prediction of acetylene peak mole fraction in the flames with PO may be reached by a refinement of the branching ratio for the reactions of PO isomerization to acetone and propanal in the flame. Particularly, according to the ROP-analysis, the presence of PO in the flame contributes to the formation of acetylene due to the chain of H-abstraction reactions with flame radicals: $C_2H_5 \rightarrow C_2H_4 \rightarrow C_2H_3 \rightarrow C_2H_2$. Therefore, an increase in the $k_{acetone}/k_{propanal}$ ratio (isomerization reaction rate constants of PO to acetone and propanal, respectively) could probably decrease the predicted peak mole fraction of acetylene in the flames with PO additive. This hypothesis is supported by the fact that in the burner-stabilized flames of acetone, a lower mole fraction of acetylene is formed as compared to the flame fuelled by propanal in similar flame conditions.[60] We varied the ratio of pre-exponential factors of $k_{acetone}$ and $k_{propanal}$ within 2 orders of magnitude in the mechanism C3Mech; however, no notable change in the predicted C_2H_2 peak mole fraction as compared to unmodified C3Mech was observed. This, most likely, is related to too low C_2H_2 sensitivity to the reactions R154 and R130 (Figure 10),

Figure 10. Sensitivity coefficients of C_2H_2 peak mole fraction (C3Mech).

and also related to the conversion of ethane to ethyl radicals via H-abstraction reactions.

As was mentioned above and as seen from Figure 10, another option suggesting an improvement of C_2H_2 prediction in the flames (particularly, in the postflame zone) is a revision of key reactions responsible for acetylene consumption and production in the core hydrocarbon mechanism. To reveal such reactions in different zones of the flame, we analyzed the C_2H_2 sensitivities at various heights above the burner, and they are depicted in Figure 11.
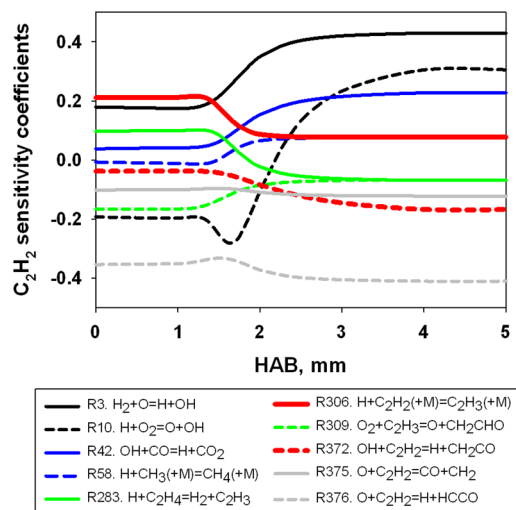

Figure 11. Sensitivity coefficients of C_2H_2 in Flame D (according to C3Mech).

As seen, for most reactions, the sensitivity coefficient of C_2H_2 strongly depends on the height above the burner; therefore, reconsidering the rate constants of the reactions, the sensitivity of which is different in the high and low temperature zones of the flame, is needed to improve the model in its prediction of C_2H_2 across the flame zone. Among these reactions, there are the reactions whose rate constants were extensively studied in the literature and reliably evaluated, and they are the following: the chain branching reactions (R3, R10), the key heat release reaction (R42), the reaction of vinyl radical with O_2 (R309), and the reaction of H abstraction from ethylene (R283). Therefore, in this work, we paid a particular attention to the rate constant parameters of only some of the reactions shown in Figure 11 and also listed in Table 2.

For the reaction of C_2H_3 consumption (R306), the rate constant parameters suggested by Miller and Klippenstein[61] are used in C3Mech. However, Ma et al.[62] in their study of premixed ethylene flames used the rate constant for this reaction as suggested in a more recent investigation of Wang et al.,[63] who proposed using its direct approximation via Chebyshev expansion[64] to yield a more reliable and accurate dependence on pressure and temperature. The rate constant parameters for the reaction R372 used in the C3Mech are taken from the work of Senosiain et al.[65] However, in a more recent study, Liu et al.[57] suggested a new rate coefficient expression formulated by regressing the available experimental data for this reaction rate constant in high temperature region.

Thus, we modified the C3Mech mechanism by adopting the updated rate constant parameters for the reaction R306 and R372 from the works of Wang et al.[63] and Liu et al.,[57] respectively. Moreover, in the modified mechanism, for the reaction R58, we used the rate constant recently measured by Wang et al.,[67] and for the reactions of C_2H_2 with O (R375 and R376), we adopted the rate constants from the LLNL detailed mechanism for n-heptane combustion.[66] The C3Mech with the modifications mentioned above is available in CHEMKIN format in the Supporting Information. The comparisons of the predictions of C_2H_2 and selected PAHs mole fraction profiles using the original C3Mech and its modified version (C3Mech_mod) in the base flame (Flame A) and the flame with 8.9% PO in fuel (Flame D) are presented in Figures 12−13.

As seen from Figure 12, the revision of the above-mentioned reaction rate constants results in a decreased peak and

Table 2. List of Reactions Modified in C3Mech to Refine Prediction of Acetylene Mole Fraction Profile in the Flames

|		rate constant in modified Arrhenius form $k = AT^n\exp(-E_a/RT)$, the units are K, s^{-1}, cm^3 and cal/mol				
no.	reaction	A	n	E	ref	
R372	$OH+C_2H_2 = H+CH_2CO$	1.33×10^{13}	0.11	11059	57	
R375	$C_2H_2+O = CH_2+CO$	6.120×10^{06}	2.00	1.900×10^{03}	66	
		rev/1.152×10^{06}	2.00	5.257×10^{04}/		
R376	$C_2H_2+O = HCCO+H$	1.430×10^{07}	2.00	1.900×10^{03}	66	
		rev/2.021×10^{05}	2.00	1.331×10^{04} /		
R58	$CH_4(+M) = CH_3+H(+M)$	2.10×10^{16}	0.00	104913.6	67	
		LOW/3.91×10^{17}	0.00	89812.4/		
		TROE/0.50 1350 1350 7834 /				
		rate constant in Chebyshev format[64]				
R306	$H+C_2H_2 (+M) = C_2H_3 (+M)$		1.00	0.0	0.0	62
	TCHEB /			500.0	2000.0 /	
	PCHEB /			1.00×10^{-03}	1.00×10^{02} /	
	CHEB/7 4 $1.0631 \times 10^{01} 2.2524 \times 10^{00} -1.5114 \times 10^{-01} -6.3036 \times 10^{-02}$/					
	CHEB/ $-3.3509 \times 10^{-01} 2.4814 \times 10^{-01} 1.4262 \times 10^{-01} 4.8996 \times 10^{-02} -3.5145 \times 10^{-01}$/					
	CHEB/ $-5.9670 \times 10^{-03} 3.3570 \times 10^{-03} 8.6600 \times 10^{-03} -9.3740 \times 10^{-02} -9.5393 \times 10^{-03}$/					
	CHEB/ $-5.4786 \times 10^{-03} -9.9965 \times 10^{-04} -2.0417 \times 10^{-02} -2.9275 \times 10^{-03} -2.2531 \times 10^{-03}$/					
	CHEB/ $-1.2784 \times 10^{-03} -2.2207 \times 10^{-03} -3.0803 \times 10^{-04} -3.5237 \times 10^{-04} -3.7207 \times 10^{-04}$/					
	CHEB/$8.8859 \times 10^{-04} 2.4405 \times 10^{-04} 1.2987 \times 10^{-04} 1.4597 \times 10^{-05}$/					
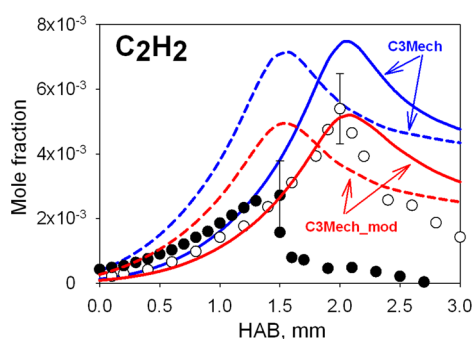
Figure 12. Acetylene mole fraction profiles measured and predicted by the original and modified (see text) C3Mech. Open symbols and solid lines: base flame (Flame A); filled symbols and dashed lines: flame with 8.9%PO in fuel (Flame D).

postflame mole fraction of acetylene in the flames with and without PO and therefore leads to a better agreement with experimental data. Nevertheless, the modified mechanism, as well as the original one, overpredicts C_2H_2 peak mole fraction in the flame with addition of PO. It is interesting that previous studies of the effect of oxygenates on the chemical speciation of atmospheric-pressure premixed hydrocarbon flames (particularly, ethanol to ethylene,[34] and methyl pentanoate to *n*-heptane/toluene mixture[30]) also showed a strong inhibiting influence of the oxygenates on the peak mole fraction of acetylene in the flames, which was underpredicted by detailed kinetic models. Summarizing these findings, one can conclude that the observed discrepancy may be related to an inability of kinetic mechanisms to accurately predict O atoms' concentration (especially in the flames of oxygenated fuels), which are involved in the reactions of acetylene consumption. Low concentrations of atomic oxygen in fuel-rich conditions and difficulties encountered by experimentalists in its measurements (they were mentioned in Section 4.3) do not allow an

adequate validation of the core kinetic mechanisms against the O measurements in flames, which are fairly scarce, see, e.g.[68,69]

The revisions made to the C3Mech resulted in negligibly slight changes in the mole fraction profiles of small hydrocarbons and small PAHs (with 1−3 aromatic rings), however, led to some improvements in prediction of methane profiles (they are shown in Figure S5). Figure 13 exemplarily demonstrates the predicted mole fraction profiles of phenanthrene (3 aromatic rings, $C_{14}H_{10}$), which is formed in the reaction involving (but not limited to) acetylene and biphenyl radical (Figure S1). Both modified and unmodified mechanisms predict very similar phenanthrene profiles in Flame A and Flame D, and the effect of PO addition is very weak according to the modeling. As also seen from Figure 13, the effect of acetylene chemistry is more significant on pyrene (4 aromatic rings) mole fraction profiles: the modified mechanism predicts a lower peak mole fraction of this species in both flames. Noteworthy that the updated acetylene chemistry has a substantial influence on the predicted mole fraction profiles of $C_{18}H_{10}$ and $C_{20}H_{10}$, also shown in Figure 13: their mole fractions predicted by the modified mechanism are up to ~75% lower than those calculated using the original mechanism. Since formation of a particular PAH proceeds via several steps of C_2H_2 addition, the production of heavier PAH molecules becomes more sensitive to C_2H_2 concentration.

Therefore, Figures 12 and 13 clearly demonstrate that accurate prediction of acetylene is vital for adequate reproducing the mole fraction profiles of PAHs. The fact that the kinetic mechanism significantly underestimates the effect of PO additive on C_2H_2 peak mole fraction indicates indirectly that the mechanism is expected to significantly overpredict the heavy PAHs (4 and more aromatic rings) in the flames with PO. We were not able in this work to measure these PAH species using our experimental setup to verify this modeling result. However, it should be noted that these compounds are usually very difficult to measure due to their
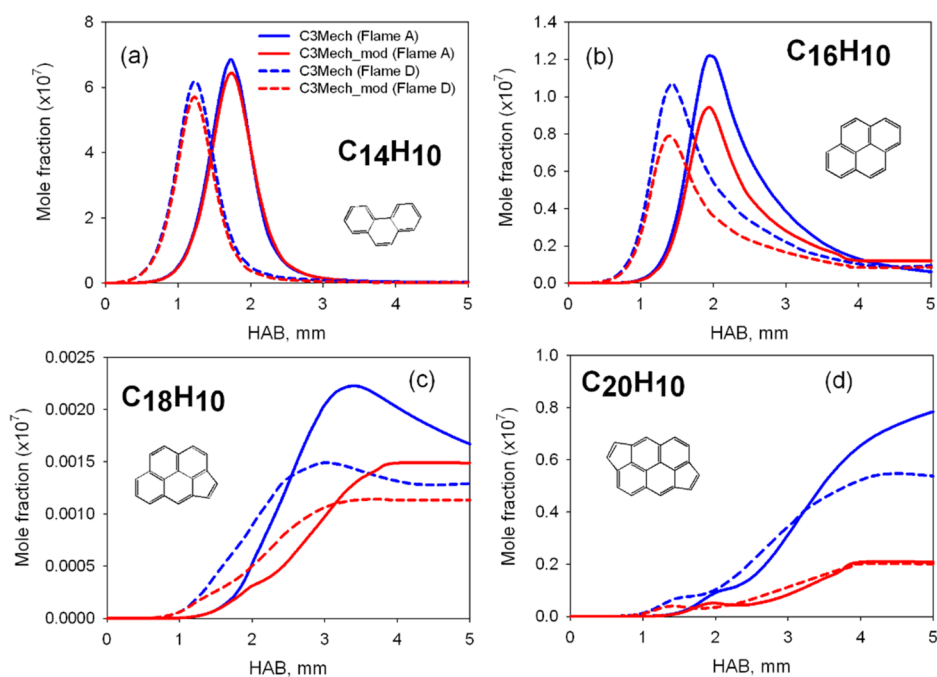

Figure 13. Mole fraction profiles of selected PAHs predicted by the original and modified C3Mech.

low concentrations and therefore their observations in the flames are very scarce in literature, see e.g.[70,71] The measurements of heavy PAHs in the flames fueled by the mixtures of hydrocarbons with propylene oxide are thus needed to further validate and improve the PAH formation submechanism in the available kinetic models for cocombustion of oxygenates and hydrocarbon fuels.

5. CONCLUSIONS

In this work, flame sampling molecular beam mass spectrometry was used to obtain new experimental data on the chemical speciation of laminar premixed fuel-rich (ϕ = 1.6) burner-stabilized flames fueled by n-heptane/toluene mixture (7:3 by volume of liquids) with and without addition of propylene oxide. In total, the chemical structures of 5 flames with various loading of PO in the unburnt gas (from 0% to 16.3% in fuel mixture in mole basis) were studied. Spatial distributions of mole fractions of reactants, major products, and some intermediates (small hydrocarbons, some major flame radicals and aromatic species) above the burner were measured. Three detailed kinetic mechanisms were validated against the measurement data: CRECK, C3Mech (both are available in the literature), and D+K mechanism (developed by merging the mechanism of Dirrenberger et al.,[29] and the propylene oxide chemistry adopted from the work of Capriolo et al.[51]). All three mechanisms have been shown to perform generally well in reproducing the measurements, however, some quantitative discrepancies between predictions and observations were found.

According to both modeling and experiment, addition of propylene oxide to the base fuel results in a higher reactivity of the mixture and also in a reduction of the peak mole fraction of aromatic intermediates (benzene, styrene, ethyl benzene, phenol). Analysis of the reaction pathways of formation of these intermediates showed that their reduction in the flame with PO is due to simultaneously two factors: (1) the partial replacement of "sooting" fuel (toluene, which is the main precursor of these species) with oxygenated additive, and (2) the changes in the flame radical pool caused by PO addition. Propylene oxide additive was found to change the ratio between H, OH, O, and CH_3 toward an increase in the proportion of O and CH_3. This in turn affects the concentrations of other hydrocarbon intermediates in the flame.

All tested kinetic mechanisms were found to underestimate the effect of PO additive on the peak mole fractions of methane, acetylene, ethylene, allene+propyne and diacetylene. Since acetylene is an intermediate playing a key role in PAH growth, its chemistry was revisited in order to provide a better prediction of PAHs. The sensitivity analysis for C_2H_2 and the ROP analysis of PO oxidation pathways have shown that PO contributes to the formation of acetylene due to favoring the rapid production of CH_3, C_2H_5 and HCO radicals. Since primary products of PO transformation in the flame are propanal and acetone, these two intermediates serve as precursors of HCO and C_2H_5 (propanal), and CH_3 (acetone). This allowed concluding that a variation of the branching ratio for the reactions of PO isomerization to acetone and propanal may have an effect on the predicted C_2H_2 mole fraction. However, this hypothesis was not confirmed. The sensitivity analysis allowed revealing the reactions playing a key role in acetylene formation and consumption. Their rate constant parameters were updated in the C3Mech, as the most detailed

mechanism including heavy PAHs, according to the recent findings in literature. The modified C3Mech was shown to have a better predictive ability of acetylene mole fraction profiles in the flames with and without PO.

The revisions made to the mechanism substantially affected on the predicted mole fraction profiles of PAHs with 4 aromatic rings and heavier ones ($C_{18}H_{10}$ and $C_{20}H_{10}$) clearly demonstrating that a more accurate prediction of acetylene is vital for adequate reproducing the mole fraction profiles of PAHs. The measurement data reported in this work extend the available experimental data in the literature for combustion of propylene oxide and its cofiring with diesel fuel surrogate, and can be used as a guidance for further refinement of the submechanisms for PO combustion and PAH formation.

■ ASSOCIATED CONTENT

ⓢ Supporting Information

The Supporting Information is available free of charge at https://pubs.acs.org/doi/10.1021/acsomega.2c05999.

Tabulated experimental data (profiles of temperature and species mole fractions) (XLSX)

Files of the modified C3Mech mechanism in CHEM-KIN format (ZIP)

Supplementary figures (Figures S1−S5) and Table S1 (PDF)

■ AUTHOR INFORMATION

Corresponding Author

Denis A. Knyazkov − *Voevodsky Institute of Chemical Kinetics and Combustion, Novosibirsk 630090, Russia;* ⓞ orcid.org/0000-0002-6819-4935; Email: knyazkov@kinetics.nsc.ru

Authors

Artëm M. Dmitriev − *Voevodsky Institute of Chemical Kinetics and Combustion, Novosibirsk 630090, Russia;* ⓞ orcid.org/0000-0002-0162-7636

Ksenia N. Osipova − *Voevodsky Institute of Chemical Kinetics and Combustion, Novosibirsk 630090, Russia;* ⓞ orcid.org/0000-0001-5025-033X

Andrey G. Shmakov − *Voevodsky Institute of Chemical Kinetics and Combustion, Novosibirsk 630090, Russia;* ⓞ orcid.org/0000-0001-6810-7638

Complete contact information is available at:
https://pubs.acs.org/10.1021/acsomega.2c05999

Notes

The authors declare no competing financial interest.

■ REFERENCES

(1) Li, H.; Abraham, C. S.; Anand, M.; Cao, A.; Nørskov, J. K. Opportunities and Challenges in Electrolytic Propylene Epoxidation. *J. Phys. Chem. Lett.* **2022**, *13* (9), 2057−2063.

(2) Kizilkaya, A. C.; Fellah, M. F.; Onal, I. Direct Gas-Phase Epoxidation of Propylene to Propylene Oxide through Radical Reactions: A Theoretical Study. *Chem. Phys. Lett.* **2010**, *487* (4), 183−189.

(3) Hayashi, T.; Tanaka, K.; Haruta, M. Selective Vapor-Phase Epoxidation of Propylene over Au/TiO2Catalysts in the Presence of Oxygen and Hydrogen. *J. Catal.* **1998**, *178* (2), 566−575.

(4) Clerici, M. G.; Bellussi, G.; Romano, U. Synthesis of Propylene Oxide from Propylene and Hydrogen Peroxide Catalyzed by Titanium Silicalite. *J. Catal.* **1991**, *129* (1), 159−167.

(5) Peng, J.; Wan, Z.; Chen, W.; Hu, H.; Huang, Q.; Chen, X. Theoretical Comparative Study on the Mechanism of Gas Phase Epoxidation of Propylene about Complete and Defective Dimer MoOx. *Computational and Theoretical Chemistry* **2022**, *1210*, 113641.

(6) Lei, Y.; Mehmood, F.; Lee, S.; Greeley, J.; Lee, B.; Seifert, S.; Winans, R. E.; Elam, J. W.; Meyer, R. J.; Redfern, P. C.; Teschner, D.; Schlögl, R.; Pellin, M. J.; Curtiss, L. A.; Vajda, S. Increased Silver Activity for Direct Propylene Epoxidation via Subnanometer Size Effects. *Science* **2010**, *328* (5975), 224−228.

(7) Khan, F. I.; Abbasi, S. A. An Assessment of the Likelihood of Occurrence, and the Damage Potential of Domino Effect (Chain of Accidents) in a Typical Cluster of Industries. *Journal of Loss Prevention in the Process Industries* **2001**, *14* (4), 283−306.

(8) Liu, L.; Zhang, Q. Flame Range and Energy Output in Two-Phase Propylene Oxide/Air Mixtures beyond the Original Premixed Zone. *Energy* **2019**, *171*, 666−677.

(9) Liu, L.; Zhang, Q. Comparison of Detonation Characteristics for Typical Binary Blended Fuel. *Fuel* **2020**, *268*, 117351.

(10) Ye, C.; Du, Q.; Liu, L.; Zhang, Q.Flame Behavior, Shock Wave, and Instantaneous Thermal Field Generated by Unconfined Vapor-Liquid Propylene Oxide/Air Cloud Detonation. *Defence Technology***2022**. DOI: 10.1016/j.dt.2022.05.002.

(11) Du, Q.; Liang, H.; Zhang, Q. Hazards of Propylene Oxide Aerosols in the Secondary Explosion. *Combust. Sci. Technol.* **2021**, *0* (0), 1−16.

(12) Burke, S. M.; Metcalfe, W.; Herbinet, O.; Battin-Leclerc, F.; Haas, F. M.; Santner, J.; Dryer, F. L.; Curran, H. J. An Experimental and Modeling Study of Propene Oxidation. Part 1: Speciation Measurements in Jet-Stirred and Flow Reactors. *Combust. Flame* **2014**, *161* (11), 2765−2784.

(13) Ramalingam, A.; Fenard, Y.; Heufer, A. Ignition Delay Time and Species Measurement in a Rapid Compression Machine: A Case Study on High-Pressure Oxidation of Propane. *Combust. Flame* **2020**, *211*, 392−405.

(14) Lifshitz, A.; Tamburu, C. Isomerization and Decomposition of Propylene Oxide. Studies with a Single-Pulse Shock Tube. *J. Phys. Chem.* **1994**, *98* (4), 1161−1170.

(15) Burluka, A. A.; Harker, M.; Osman, H.; Sheppard, C. G. W.; Konnov, A. A. Laminar Burning Velocities of Three C3H6O Isomers at Atmospheric Pressure. *Fuel* **2010**, *89* (10), 2864−2872.

(16) Knyazkov, D. A.; Dmitriev, A. M.; Korobeinichev, O. P.; Osipova, K. N.; Pio, G.; Shmakov, A. G.; Salzano, E. Structure of Premixed Flames of Propylene Oxide: Molecular Beam Mass Spectrometric Study and Numerical Simulation. *Proceedings of the Combustion Institute* **2021**, *38* (2), 2467−2475.

(17) Ramalingam, A.; Minwegen, H.; Fenard, Y.; Heufer, K. A. Insights into the Oxidation of Propylene Oxide through the Analysis of Experiments and Kinetic Modeling. *Proceedings of the Combustion Institute* **2021**, *38* (1), 459−467.

(18) Miroshnikov, A. M.; Tsygankov, D. V. Mechanism of Action of Oxygenates. *Chem. Technol. Fuels Oils* **2009**, *45* (3), 177−182.

(19) Tsygankov, D. V.; Miroshnikov, A. M.; Grishaeva, A. M. Determination of Mutual Solubility in the Straight-Run Naphtha—Propylene Oxide—Water System. *Chem. Technol. Fuels Oils* **2011**, *47* (1), 28−33.

(20) Sweeney, L. M.; Kirman, C. R.; Albertini, R. J.; Tan, Y.-M.; Clewell, H. J.; Filser, J. G.; Csanády, G.; Pottenger, L. H.; Banton, M. I.; Graham, C. J.; Andrews, L. S.; Papciak, R. J.; Gargas, M. L. Derivation of Inhalation Toxicity Reference Values for Propylene Oxide Using Mode of Action Analysis: Example of a Threshold Carcinogen. *Critical Reviews in Toxicology* **2009**, *39* (6), 462−486.

(21) Awad, O. I.; Mamat, R.; Ibrahim, T. K.; Hammid, A. T.; Yusri, I. M.; Hamidi, M. A.; Humada, A. M.; Yusop, A. F. Overview of the Oxygenated Fuels in Spark Ignition Engine: Environmental and Performance. *Renewable and Sustainable Energy Reviews* **2018**, *91*, 394−408.

(22) Yang, B.; Sun, W.; Moshammer, K.; Hansen, N. Review of the Influence of Oxygenated Additives on the Combustion Chemistry of Hydrocarbons. *Energy Fuels* **2021**, *35*, 13550.

(23) Westbrook, C. K.; Pitz, W. J.; Curran, H. J. Chemical Kinetic Modeling Study of the Effects of Oxygenated Hydrocarbons on Soot Emissions from Diesel Engines. *J. Phys. Chem. A* **2006**, *110* (21), 6912−6922.

(24) Pepiot-Desjardins, P.; Pitsch, H.; Malhotra, R.; Kirby, S. R.; Boehman, A. L. Structural Group Analysis for Soot Reduction Tendency of Oxygenated Fuels. *Combust. Flame* **2008**, *154* (1), 191−205.

(25) Graziano, B.; Burkardt, P.; Neumann, M.; Pitsch, H.; Pischinger, S. Development of a Modified Joback−Reid Group Contribution Method to Predict the Sooting Tendency of Oxygenated Fuels. *Energy Fuels* **2021**, *35*, 13144.

(26) Lemaire, R.; Le Corre, G.; Nakouri, M. Predicting the Propensity to Soot of Hydrocarbons and Oxygenated Molecules by Means of Structural Group Contribution Factors Derived from the Processing of Unified Sooting Indexes. *Fuel* **2021**, *302*, 121104.

(27) Xu, L.; Wang, Y.; Liu, D. Effects of Oxygenated Biofuel Additives on Soot Formation: A Comprehensive Review of Laboratory-Scale Studies. *Fuel* **2022**, *313*, 122635.

(28) Xu, H.; Yao, C.; Xu, G.; Wang, Z.; Jin, H. Experimental and Modelling Studies of the Effects of Methanol and Ethanol Addition on the Laminar Premixed Low-Pressure n-Heptane/Toluene Flames. *Combust. Flame* **2013**, *160* (8), 1333−1344.

(29) Dirrenberger, P.; Glaude, P. A.; Bounaceur, R.; Le Gall, H.; da Cruz, A. P.; Konnov, A. A.; Battin-Leclerc, F. Laminar Burning Velocity of Gasolines with Addition of Ethanol. *Fuel* **2014**, *115*, 162−169.

(30) Dmitriev, A. M.; Knyazkov, D. A.; Bolshova, T. A.; Shmakov, A. G.; Korobeinichev, O. P. The Effect of Methyl Pentanoate Addition on the Structure of Premixed Fuel-Rich n-Heptane/Toluene Flame at Atmospheric Pressure. *Combust. Flame* **2015**, *162* (5), 1964−1975.

(31) Osipova, K. N.; Bolshova, T. A.; Korobeinichev, O. P.; Kuibida, L. V.; Shmakov, A. G. Effect of Addition of Methyl Hexanoate and Ethyl Pentanoate on the Structure of Premixed N-Heptane/Toluene/O2/Ar Flame. *Energy Fuels* **2019**, *33* (5), 4585−4597.

(32) Botha, J. P.; Spalding, D. B. The Laminar Flame Speed of Propane/Air Mixtures with Heat Extraction from the Flame. *Proceedings of the Royal Society of London. Series A. Mathematical and Physical Sciences* **1954**, *225* (1160), 71−96.

(33) Knyazkov, D. A.; Slavinskaya, N. A.; Dmitriev, A. M.; Shmakov, A. G.; Korobeinichev, O. P.; Riedel, U. Structure of an N-Heptane/Toluene Flame: Molecular Beam Mass Spectrometry and Computer Simulation Investigations. *Combust Explos Shock Waves* **2016**, *52* (2), 142−154.

(34) Gerasimov, I. E.; Knyazkov, D. A.; Yakimov, S. A.; Bolshova, T. A.; Shmakov, A. G.; Korobeinichev, O. P. Structure of Atmospheric-Pressure Fuel-Rich Premixed Ethylene Flame with and without Ethanol. *Combust. Flame* **2012**, *159* (5), 1840−1850.

(35) Gerasimov, I. E.; Knyazkov, D. A.; Bolshova, T. A.; Shmakov, A. G.; Korobeinichev, O. P.; Carbonnier, M.; Lefort, B.; Kéromnès, A.; Le Moyne, L.; Lubrano Lavadera, M.; Konnov, A. A.; Zhou, C.-W.; Serinyel, Z.; Dayma, G.; Dagaut, P. Methyl-3-Hexenoate Combustion Chemistry: Experimental Study and Numerical Kinetic Simulation. *Combust. Flame* **2020**, *222*, 170−180.

(36) Knyazkov, D. A.; Bolshova, T. A.; Dmitriev, A. M.; Shmakov, A. G.; Korobeinichev, O. P. The Effect of Methyl Pentanoate Addition on the Structure of a Non-Premixed Counterflow n-Heptane/O2 Flame. *Energy Fuels* **2018**, *32*, 2397.

(37) Shmakov, A. G.; Knyazkov, D. A.; Bolshova, T. A.; Dmitriev, A. M.; Korobeinichev, O. P. Effect of CO2 Addition on the Structure of Premixed Fuel-Rich CH4/O2/N2 and C3H8/O2/N2 Flames Stabilized on a Flat Burner at Atmospheric Pressure. *Energy Fuels* **2016**, *30* (3), 2395−2406.

(38) Cool, T. A.; Nakajima, K.; Taatjes, C. A.; McIlroy, A.; Westmoreland, P. R.; Law, M. E.; Morel, A. Studies of a Fuel-Rich Propane Flame with Photoionization Mass Spectrometry. *Proceedings of the Combustion Institute* **2005**, *30* (1), 1681−1688.

(39) He, X.; Giese, M.; Ruwe, L.; Lucassen, A.; Moshammer, K. A Detailed Uncertainty Analysis of EI-MBMS Data from Combustion Experiments. *Combust. Flame* **2022**, *243*, 112012.

(40) Deng, L.; Kempf, A.; Hasemann, O.; Korobeinichev, O. P.; Wlokas, I. Investigation of the Sampling Nozzle Effect on Laminar Flat Flames. *Combust. Flame* **2015**, *162* (5), 1737−1747.

(41) Skovorodko, P. A.; Tereshchenko, A. G.; Korobeinichev, O. P.; Knyazkov, D. A.; Shmakov, A. G. Experimental and Numerical Study of Probe-Induced Perturbations of the Flame Structure. *Combustion Theory and Modelling* **2013**, *17* (1), 1−24.

(42) Hansen, N.; Cool, T. A.; Westmoreland, P. R.; Kohse-Höinghaus, K. Recent Contributions of Flame-Sampling Molecular-Beam Mass Spectrometry to a Fundamental Understanding of Combustion Chemistry. *Prog. Energy Combust. Sci.* **2009**, *35* (2), 168−191.

(43) Hansen, N.; Tranter, R. S.; Randazzo, J. B.; Lockhart, J. P. A.; Kastengren, A. L. Investigation of Sampling-Probe Distorted Temperature Fields with X-Ray Fluorescence Spectroscopy. *Proceedings of the Combustion Institute* **2019**, *37* (2), 1401−1408.

(44) Knyazkov, D. A.; Gerasimov, I. E.; Bolshova, T. A.; Kiselev, V. G.; Shmakov, A. G.; Paletsky, A. A. Cationic Structure of Premixed Near-Stoichiometric CH4/O2/Ar Flames at Atmospheric Pressure: New Insights from Mass Spectrometry, Quantum Chemistry, and Kinetic Modeling. *Submitted to Combustion and Flame* **2022**, *241*, 112106.

(45) Karakaya, Y.; Sellmann, J.; Wlokas, I.; Kasper, T. Influence of the Sampling Probe on Flame Temperature, Species, Residence Times and on the Interpretation of Ion Signals of Methane/Oxygen Flames in Molecular Beam Mass Spectrometry Measurements. *Combust. Flame* **2021**, *229*, 111388.

(46) Dmitriev, A. M.; Knyazkov, D. A.; Bolshova, T. A.; Tereshchenko, A. G.; Paletsky, A. A.; Shmakov, A. G.; Korobeinichev, O. P. Structure of CH4/O2/Ar Flames at Elevated Pressures Studied by Flame Sampling Molecular Beam Mass Spectrometry and Numerical Simulation. *Combust. Flame* **2015**, *162* (10), 3946−3959.

(47) Kaskan, W. E. The Dependence of Flame Temperature on Mass Burning Velocity. *Proceedings of the Combustion Institute* **1957**, *6* (1), 134−143.

(48) Shaddix, C. R.Correcting Thermocouple Measurements for Radiation Loss: A Critical Review. In *Proceedings of the 33rd National Heat Transfer Conference NHTC'99*; Jensen, M. K., Di Marzo, M., Eds.; Sandia National Labs: Livermore, CA, 1999.

(49) Ranzi, E.; Frassoldati, A.; Grana, R.; Cuoci, A.; Faravelli, T.; Kelley, A. P.; Law, C. K. Hierarchical and Comparative Kinetic Modeling of Laminar Flame Speeds of Hydrocarbon and Oxygenated Fuels. *Prog. Energy Combust. Sci.* **2012**, *38* (4), 468−501.

(50) Dong, S.; Wagnon, S. W.; Pratali Maffei, L.; Kukkadapu, G.; Nobili, A.; Mao, Q.; Pelucchi, M.; Cai, L.; Zhang, K.; Raju, M.; Chatterjee, T.; Pitz, W. J.; Faravelli, T.; Pitsch, H.; Senecal, P. K.; Curran, H. J. A New Detailed Kinetic Model for Surrogate Fuels: C3MechV3.3. *Applications in Energy and Combustion Science* **2022**, *9*, 100043.

(51) Capriolo, G.; Alekseev, V. A.; Konnov, A. A. An Experimental and Kinetic Study of Propanal Oxidation. *Combust. Flame* **2018**, *197*, 11−21.

(52) Lin, K. C.; Lee, T.-W. Skeletal Mechanism of Ethyl Propionate Oxidation for CFD Modeling to Predict Experimental Profiles of Unsaturated Products in a Nonpremixed Flame. *Energy Fuels* **2018**, *32* (1), 855−866.

(53) Pio, G.; Palma, V.; Salzano, E. Comparison and Validation of Detailed Kinetic Models for the Oxidation of Light Alkenes. *Ind. Eng. Chem. Res.* **2018**, *57* (21), 7130−7135.

(54) Reizer, E.; Viskolcz, B.; Fiser, B. Formation and Growth Mechanisms of Polycyclic Aromatic Hydrocarbons: A Mini-Review. *Chemosphere* **2022**, *291*, 132793.

(55) Osipova, K. N.; Dmitriev, A. M.; Shmakov, A. G.; Korobeinichev, O. P.; Minaev, S. S.; Knyazkov, D. A. Combustion of Ethyl Acetate: The Experimental Study of Flame Structure and Validation of Chemical Kinetic Mechanisms. *Mendeleev Commun.* **2019**, *29* (6), 690−692.

(56) Li, Y.; Cai, J.; Zhang, L.; Yuan, T.; Zhang, K.; Qi, F. Investigation on Chemical Structures of Premixed Toluene Flames at Low Pressure. *Proceedings of the Combustion Institute* **2011**, *33* (1), 593−600.

(57) Liu, Y.; Zhang, Q.; Wang, T. Detailed Chemistry Modeling of Partial Combustion of Natural Gas for Coproducing Acetylene and Syngas. *Combust. Sci. Technol.* **2017**, *189* (5), 908−922.

(58) Frenklach, M.; Mebel, A. M. On the Mechanism of Soot Nucleation. *Phys. Chem. Chem. Phys.* **2020**, *22* (9), 5314−5331.

(59) Georganta, E.; Rahman, R. K.; Raj, A.; Sinha, S. Growth of Polycyclic Aromatic Hydrocarbons (PAHs) by Methyl Radicals: Pyrene Formation from Phenanthrene. *Combust. Flame* **2017**, *185*, 129−141.

(60) Liao, H.; Tao, T.; Sun, W.; Hansen, N.; Yang, B. Isomer-Specific Speciation Behaviors Probed from Premixed Flames Fueled by Acetone and Propanal. *Proceedings of the Combustion Institute* **2021**, *38* (2), 2441−2448.

(61) Miller, J. A.; Klippenstein, S. J. The H + C2H2 (+M) ⇄ C2H3 (+M) and H + C2H2 (+M) ⇄ C2H5 (+M) Reactions: Electronic Structure, Variational Transition-State Theory, and Solutions to a Two-Dimensional Master Equation. *Phys. Chem. Chem. Phys.* **2004**, *6* (6), 1192−1202.

(62) Ma, S.; Zhang, X.; Dmitriev, A.; Shmakov, A.; Korobeinichev, O.; Mei, B.; Li, Y.; Knyazkov, D. Revisit Laminar Premixed Ethylene Flames at Elevated Pressures: A Mass Spectrometric and Laminar Flame Propagation Study. *Combust. Flame* **2021**, *230*, 111422.

(63) Wang, K.; Villano, S. M.; Dean, A. M. Experimental and Kinetic Modeling Study of Butene Isomer Pyrolysis: Part I. 1- and 2-Butene. *Combust. Flame* **2016**, *173*, 347−369.

(64) Venkatesh, P. K.; Chang, A. Y.; Dean, A. M.; Cohen, M. H.; Carr, R. W. Parameterization of Pressure- and Temperature-Dependent Kinetics in Multiple Well Reactions. *AIChE J.* **1997**, *43* (5), 1331−1340.

(65) Senosiain, J. P.; Klippenstein, S. J.; Miller, J. A. The Reaction of Acetylene with Hydroxyl Radicals. *J. Phys. Chem. A* **2005**, *109* (27), 6045−6055.

(66) Mehl, M.; Pitz, W. J.; Westbrook, C. K.; Curran, H. J. Kinetic Modeling of Gasoline Surrogate Components and Mixtures under Engine Conditions. *Proceedings of the Combustion Institute* **2011**, *33* (1), 193−200.

(67) Wang, S.; Davidson, D. F.; Hanson, R. K. Improved Shock Tube Measurement of the CH4 + Ar = CH3 + H + Ar Rate Constant Using UV Cavity-Enhanced Absorption Spectroscopy of CH3. *J. Phys. Chem. A* **2016**, *120* (28), 5427−5434.

(68) Knyazkov, D. A.; Dmitriev, A. M.; Bolshova, T. A.; Shvartsberg, V. M.; Shmakov, A. G.; Korobeinichev, O. P. Structure of Premixed H2/O2/Ar Flames at 1−5 atm Studied by Molecular Beam Mass Spectrometry and Numerical Simulation. *Proceedings of the Combustion Institute* **2017**, *36* (1), 1233−1240.

(69) Alekseev, V. A.; Bystrov, N.; Emelianov, A.; Eremin, A.; Yatsenko, P.; Konnov, A. A. High-Temperature Oxidation of Acetylene by N2O at High Ar Dilution Conditions and in Laminar Premixed C2H2 + O2 + N2 Flames. *Combust. Flame* **2022**, *238*, 111924.

(70) Li, Y.; Tian, Z.; Zhang, L.; Yuan, T.; Zhang, K.; Yang, B.; Qi, F. An Experimental Study of the Rich Premixed Ethylbenzene Flame at Low Pressure. *Proceedings of the Combustion Institute* **2009**, *32* (1), 647−655.

(71) Wartel, M.; Pauwels, J.-F.; Desgroux, P.; Mercier, X. Pyrene Measurements in Sooting Low Pressure Methane Flames by Jet-

Cooled Laser-Induced Fluorescence. *J. Phys. Chem. A* **2011**, *115* (49), 14153−14162.